Acidity and accessibility studies of desilicated ZSM-5 zeolites in terms of their effectiveness as catalysts in acid-catalyzed cracking processes

Karolina A. Tarach[a],*, Kinga Góra-Marek[a], Joaquin Martinez-Triguero[b] and Ignacio Melián-Cabrera[c,d] *

[a] Faculty of Chemistry, Jagiellonian University in Kraków, 3 Ingardena St., 30-060 Kraków, Poland, phone: +48 12 663 2081, fax: +48 12 634 0515

[b] Instituto de Tecnología Química (UPV-CSIC), Universitat Politècnica de València, Consejo Superior de Investigaciones Científicas, Av. de los Naranjos s/n 46022 Valencia, Spain

[c] Chemical Engineering Department, ITM, Faculty of Mathematics and Natural Sciences, University of Groningen Nijenborgh 4, 9747 AG Groningen, The Netherlands

[d] European Bioenergy Research Institute (EBRI), School of Engineering and Applied Science, Aston University, Aston Triangle, Birmingham B4 7ET, United Kingdom

Corresponding Authors:

* Karolina A. Tarach; P: +48(12)663 20 81; F: +48(12)634 05 15; E-mail address: karolina.tarach@uj.edu.pl

* Ignacio Melián-Cabrera; P: +44(0)121 204 3046; E-mail address: i.melian-cabrera@aston.ac.uk

Abstract

The structural, textural and acidic characteristics of hierarchical ZSM-5 (Si/Al= 18-32), obtained with two desilication approaches, and the effect of these treatments on the reactivity in various cracking reactions of variable feedstock size and severity have been investigated. Emphasis is given to understanding the accessibility of acid sites; this was investigated by textural analysis, FTIR probe molecules (pyridine, trimethylacetonitrile and 2,4,6-trimethylpyridine) and reactions involving *n*-decane, 1,3,5-triisopropylbenzene (TIPB), and low and high-density polyethylene, LDPE and HDPE, respectively. Higher surface areas and narrower pore size distribution were obtained for NaOH&TBAOH-treated materials, comparing to the NaOH-treated ones. FTIR studies of pivalonitrile and collidine adsorption correlate well with the mesopore surface area. For *n*-decane cracking activity, the acid strength is a determining factor, revealing that the NaOH&TBAOH treatment gave stronger sites than NaOH, but lower than the native zeolite. Contrarily, the TIPB cracking activity was improved by the developed mesoporosity of the alkaline treated zeolites, and this was correlated to the pivalonitrile and collidine accessibility factors. During the *n*-decane and TIPB cracking, hydrogen transfer reactions were reduced, leading to high olefin production; for the NaOH&TBAOH materials due to the shorter microporous paths after desilication. The increased acid sites accessibility leads also to an enhanced cracking activity of polyethylenes at low conversions, as determined by a decrease of the $T_{5\%}$ and $T_{50\%}$; both parameters are linearly dependent to the pivalonitrile and collidine accessibility factors, for LDPE and HDPE. The $T_{5\%}$ for HDPE is more influenced by the accessibility factors than it is for the LDPE. This is interpreted by the branching degree of HDPE and LDPE; linear HDPE is more sensitive to the enhanced amount of pore mouths of ZSM-5 channels on the mesopores. At high conversion, the influence of the $T_{50\%}$ with the accessibility factors for HDPE and LDPE is weaker, suggesting that the cracking at this stage involves intermediate molecules of smaller size with less diffusional limitations. With respect to own prior work, the chosen zeolite and the cracking of polyolefins gave more pronounced differences for the hierarchical ZSM-5.

1   Introduction

Hierarchical zeolites combining an intrinsic acidity of microporous zeolites without diffusional limitations, typical of mesoporous materials, have proven to be effective catalysts in numerous reactions [1-3]. Several different approaches concerning the synthesis and modifications have been developed to prepare hierarchically porous zeolites. The synthesis methods are gathered around two main routes: *bottom-up* methods employing templates (e.g. surfactants, porous carbons, cationic polymers, etc.)[4-7] and *top-down* approaches concerning the preferential extraction of silica or alumina from the zeolite structure [8-11]. The zeolites obtained in the presence of surfactants can be characterized by having a high concentration and strength of acid sites with uniform and usually homogeneous mesopores. On the other hand, a preferential zeolite demetalation is one of the most attractive post-synthesis modification methods in operational and costs terms. Demetallation processes not only generate the mesoporosity but also affect the acidity of hierarchical zeolite, modifying mainly the nature of the acidic sites [9,12]. Among the various post-synthesis methods, the desilication, i.e. selective silicon removal from zeolite framework, is being one of the most efficient and economic routes of mesoporosity generation. Desilicated zeolites of different types of structures and various Si/Al ratios have been reported as active catalysts[3], with effectively generated intraparticle mesoporosity. Together with the alkaline treatment, the use of pore directing agents[9,13,14] allowed for a more effective preservation of the crystallinity as well as a proper pores connectivity, followed by enhanced catalytic activity[1-3]. The so-modified zeolites demonstrated an increased acidity and accessibility of the sites responsible for a more efficient reaction yield over the catalytically active centers. Higher activity has been especially well seen in the case of bulky and branched reactants, where diffusional constraints limit the reaction occurrence only to the zeolite grains surface[3,9].

Desilicated zeolites possess features making them promising catalysts in plastic waste cracking reactions[15,16]. The recycling of plastic waste is an important environmental problem; production and post customer plastic wastes reach values of million tons, and the main disposal method is limited to landfilling[17]. The thermal pyrolysis of polymers requires high temperatures of restoring plastic waste to manufacturing lines in form of gaseous and liquid products, which can be further used as fine chemical feedstocks or fuel-like hydrocarbons. In this regard, the catalytic cracking of plastic waste can ensure lowering the temperature, higher selectivity to the desired products and a better yield of the process. Different acid porous materials have been considered as potential catalysts for the cracking of polyethylene such as silica-alumina, commercial zeolites, and mesostructured materials[17,18]. The ZSM-5 zeolite possessing strong acid sites is a highly active and selective catalyst for hydrocarbon reactions, such as cracking, isomerization and aromatization, all based on carbocation intermediates[19,20]. The microporous structure of ZSM-5 zeolite impacts the shape-selective properties hindering both the hydrogen transfer reactions and the generation of polyaromatics, what contributes to increasing the C_2–C_4 olefin selectivity with low coke generation[21]. Furthermore, the three-dimensional ZSM-5 zeolite structure entails facile diffusion of coke precursors to the outer surface of the grains, leading to high resistance toward poisoning of the active sites[22]. Nevertheless, the high viscosity and bulky molecular volume of polyethylenes require a significantly enhanced porosity, and thus the accessibility of acid sites as well. The combination of the intrinsic acidity of the zeolites with a highly developed porosity typical of mesoporous materials, both gathered in hierarchical zeolites, offer unique advantages for the catalytic cracking of polyolefinic waste plastics into fuels and chemicals.

This work focuses on a detailed investigation of the structural, textural and acidic characteristics of hierarchical ZSM-5 zeolites, obtained with different desilication approaches, and the effect of those parameters on the reactivity in various cracking reactions of variable feedstock size and severity. The presence of an external PDA (pore-directing-agent) during desilication offers a greater mesoporosity development and higher acid strength when comparing it with sodium hydroxide (NaOH) solution treatment. The interaction of PDAs with the external surface of the zeolite crystal can provide a tunable protection against zeolite dissolution, and allows for a uniform secondary mesoporosity fabrication and tailoring the acidic properties of hierarchical zeolites. Tetrapropylammonium (TPA$^+$) and soluble metal hydroxide ions [e.g., Al(OH)$_4^-$ or Ga(OH)$_4^-$], were found to be effective in directing the mesopore formation during the base leaching of highly siliceous, all-silica MFI[23] and/or USY[8]. Especially, tetraalkylammonium cations play a crucial role in making desilication more versatile and tunable[1]. The micelle-forming surfactants such as cetyltrimethylammonium (CTA$^+$), used as templates for the synthesis of ordered mesoporous materials[24-26], also induce a reassembly of the dissolved Si and Al species, previously extracted from the zeolite framework by leaching.

In particular, the desilication of a ZSM-5 zeolite by two approaches, NaOH and NaOH&TBAOH treatments, has been investigated. Physico-chemical changes were monitored by low temperature N$_2$ physisorption, TEM, SEM, XRD, XPS and ICP OES studies. Changes in acidity were followed on the basis of FTIR spectroscopy with the use of several probe molecules, which allowed the determination of the accessibility factors. The catalytic performance was investigated in the cracking of *n*-decane and 1,3,5-triisopropylbenzene (TIPB) as model reactions, as well as in the cracking of LDPE and HDPE. Linear *n*-decane easily penetrates the 10 MR channels of the ZSM-5 zeolite. Therefore the catalytic activity in *n*-decane cracking can be correlated with the strength of all acid sites. On the other hand, the performance in 1,3,5-triisopropylbenzene cracking is correlated to the accessibility of protonic sites as determined by *in-situ* FTIR studies. Finally, the accessibility studies were combined with results of the catalytic pyrolysis of LDPE and HDPE polymers. In a previous study, Tarach et al.[27] showed that the acid strength of a high-silica ZSM-5 plays a major role in the cracking of *n*-decane, while for the cracking of TIPB the mesopore surface area was more important. In the case of vacuum gas oil, the differences were less obvious than TIPB. In this study, these observations are confirmed for a high-aluminum ZSM-5. The differences between parent and hierarchical zeolites for TIPB and cracking of polyolefins are more pronounced here, highlighting the role of mesoporosity and Si/Al ratio. In terms of feedstocks of industrial importance, polyolefins gave more pronounced difference among the studied cases.

2　Experimental

2.1　Studied Materials

Parent microporous NH_4ZSM-5 of Si/Al = 32 zeolite denoted hereafter as ZSM-5/32 was supplied by Zeolyst (CP 5524G). Desilication was carried out using 0.2 M solutions of NaOH and NaOH&TBAOH (tetrabutylammonium hydroxide) mixture (TBAOH/(NaOH+TBAOH) = 0.4) at the temperature of 65 ^{o}C or 80 ^{o}C for 0.5 h or 5 h. The samples notation gives a detailed description of the applied desilication conditions, i.e. desilicating medium (NaOH or NaOH/TBAOH), temperature (°C) and treatment time (h). After desilication, the suspension was cooled down in an ice bath, filtered and washed with distillate water until neutral pH. Next fourfold Na^+/NH_4^+ ion-exchange with 0.5 M NH_4NO_3 was performed at 60 ^{o}C for 1 h. The resulting samples were filtrated, washed and dried at room temperature and finally calcined at 500 ^{o}C for 2 h.

Powdery low-density and high-density polyethylenes were kindly supplied by Sabic.

2.2　Characterization Techniques

2.2.1　Chemical analysis

Si and Al concentrations in the parent and desilicated zeolites were determined by the ICP OES method with an Optima 2100DV (PerkinElmer) spectrometer.

2.2.2　X-ray diffraction (XRD)

Wide-angle XRD patterns were taken with a Rigaku Multiflex diffractometer equipped with Cu Kα radiation (40 kV, 40 mA). Powder X-ray patterns were used for the structural identification of the relative crystallinity value (%Cryst) for all the zeolites. The determination of the relative crystallinity value was based on the intensity of the characteristic reflections in the range between 22.5 ^{o} and 25.0 ^{o}. The crystallinity of the starting zeolite was referenced at 100%.

2.2.3　X-ray photoelectron spectroscopy (XPS)

The X-ray photoelectron spectra (XPS) were measured with a Prevac photoelectron spectrometer equipped with a hemispherical VG SCIENTA R3000 analyzer. The photoelectron spectra were measured using a monochromatized aluminum AlKα source (E=1486.6 eV) and a low energy electron flood gun (FS40A-PS) to compensate the charge on the surface of nonconductive samples. The base pressure in the analysis chamber during the measurements was 5·10^{-9} mbar. Spectra were recorded with a constant pass energy of 100 eV for the survey and for high-resolution spectra. The binding energies were referenced to the Si 2p core level (103.0 eV). The surface composition and chemical environment were investigated on the basis of the peak areas and binding energies of Al 2p, Si 2p and O 1s photoelectron peaks. The fitting of high-resolution spectra was carried out by the CasaXPS software.

2.2.4　Nitrogen sorption measurements at -196 ^{o}C

Nitrogen sorption measurements were performed on a Quantachrome Autosorb-1-MP gas sorption instrument at -196 ^{o}C. Prior to the measurements, all samples were degassed under high vacuum conditions for a duration of 16 h at 350 ^{o}C. The micropore volume was calculated based on the *t*-plot

method, while the Brunauer–Emmet–Teller (BET) method was applied to determine the apparent specific surface area. The pore size distribution and mesopore volume (V_{meso}, range between 1.7 and 30 nm) were calculated via the Barrett–Joyner–Halenda (BJH) algorithm using the adsorption branch[28].

2.2.5 TEM and SEM investigations

Transmission electron microscopy was done with using a Philips CM–10 microscope operating at 100 kV. The samples under investigation were ultrasonically dispersed in 2-propanol and then transferred onto carbon-coated copper grids.

Scanning electron microscopy was done using a Philips XL 30 microscope.

2.2.6 FTIR spectroscopic studies

Prior to FTIR studies, the materials were pressed into the form of self-supporting discs (ca. 5-10 mg/cm^2) and pre-treated in situ in an IR cell at 500 ^oC under vacuum conditions for 1 hour. Spectra were recorded with a Bruker Vertex 70 spectrometer equipped with an MCT detector. The spectral resolution was set at 2 cm^{-1}. All the spectra presented in this work were normalized to 10 mg of sample. The sorption of CO (PRAXAIR 9.5) was performed at -100 ^oC up to the total saturation of the Lewis acid sites (up to maximum intensities of the 2230 cm^{-1} band) and the appearance of the bands of CO bonded to Brønsted acid sites (2175 cm^{-1}). The total concentrations of Brønsted and Lewis acid sites were determined from quantitative IR studies of pyridine (**Py**) sorption (≥ 99.8%, Sigma-Aldrich)[12,29]. Excess of Py-gas sufficient to neutralize all acid sites was adsorbed at 170 ^oC under static conditions (pressure of the Py-gas varied between 7 and 10 mbar), followed by an evacuation at the same temperature to remove the gaseous and physisorbed **Py** molecules, which was tracked by recording the spectra (until disappearance of the bands related to physisorbed phase). Subsequently, the band intensities in this spectrum were used to calculate the total concentration of Brønsted and Lewis sites. The total concentration of Brønsted and Lewis sites were calculated using the intensities (band height) of the 1545 cm^{-1} band of pyridinium ions (PyH$^+$) and the 1450 cm^{-1} band of Py coordinatively bonded to Lewis sites (PyL) by applying their respective extinction coefficients: 0.07 cm^2·µmol^{-1} for the 1545 cm^{-1} band of pyridinium ion (PyH$^+$) and 0.10 cm^2·µmol^{-1} for the 1450 cm^{-1} band of pyridine coordinatively bonded to Lewis sites (PyL).

The concentrations of the Brønsted and Lewis acid sites accessible for bulky pivalonitrile (trimethylacetonitrile) and collidine (2,4,6-trimethylpyridine), hereafter denoted as **Pn** and **Coll**, respectively, were also achieved from quantitative studies [30,31]. The pivalonitrile (98%, Sigma-Aldrich) was adsorbed on the zeolites at room temperature followed by 20 min evacuation at the same temperature, in order to remove the excess of physisorbed **Pn** probe molecules. The concentration of the Brønsted and Lewis acid sites detected by the **Pn** was calculated from the maximum intensities (band height) of the respective bands at 2277 cm^{-1} and 2305 cm^{-1} and their extinction coefficient (0.11 and 0.15 cm^2·µmol^{-1}, resp.). In the quantitative studies of collidine sorption, the zeolites were contacted with collidine (≥97%, Sigma-Aldrich) vapor at room temperature, then the physisorbed probe molecules were removed by evacuation at 200 ^oC. The concentration of the protonic sites detected by **Coll** was calculated from the maximum intensities (band height) of the CollH$^+$ bands at 1635 cm^{-1} and its extinction coefficient equals to 0.62 cm^2·µmol^{-1}.

IR quantification studies can give sometimes an overestimation of the total Al sites, compared to ICP. This can be related to the baseline subtraction, water bands compensation, etc., factors that usually affect the IR spectrum. The sample preparation for ICP OES analysis (dissolution of zeolite in HF, solution preparation) and ICP OES itself are also burdened with experimental errors.

2.3   Catalytic tests of model molecules cracking

The cracking experiments were performed in a MAT (Micro Activity Test) unit[32]. Pellets of zeolites were crushed and sieved; a fraction of the 0.59–0.84 mm was taken for cracking reactions. Catalytic experiments were carried out preserving the amount of catalyst (cat) constant and varying the feeds amounts (oil). Three cracking reactions with different cat-to-oil ratios of 1,3,5-triisopropylbenzene (TIPB) were performed at 500 $^{\circ}$C and for 60 s time on stream (TOS), with 200 mg of catalyst. For *n*-decane cracking at 500 $^{\circ}$C and for 60 s TOS, 300 mg of catalyst was diluted with 2.5 g of inert silica, and four cracking reactions with different cat-to-oil ratios were performed.

Rate constants (*k*) were calculated by fitting the conversions (X) to a first-order kinetic equation for a plug flow reactor (1) for *n*-decane and TIPB, assuming that the deactivation is enclosed in the kinetic constant and taking into account the volumetric expansion factor (2),

$$k =-(cat\ oil^{-1}TOS)^{-1}[\varepsilon X+(1+\varepsilon)\ ln(1-X)] \tag{1}$$

$$\varepsilon =(\Sigma molar\ selectivities\ of\ products)-1 \tag{2}$$

2.4   Catalytic tests of LDPE and HDPE cracking

The catalytic cracking of low-density and high-density polyethylenes (PEs) was evaluated by thermogravimetric analysis in a Mettler-Toledo TGA/SDTA851e analyzer. A stock mixture of the ground polymer and the zeolite powder was prepared in a ratio of polymer : zeolite = 3 : 1; this was prepared by intimately mixing in an agate mortar. A certain portion of the mixture (typically 5-10 mg) was loaded in a 70 µl α-Al$_2$O$_3$ crucible and weighted with a 5-digits Mettler Toledo balance before the analysis. The sample was placed in the furnace, the analytic gas was switched on and the temperature was raised from 30 to 600 $^{\circ}$C at a heating rate of 5 $^{\circ}$C /min under a nitrogen flow of 80 mL/min STP. The conversion was calculated by deducting the catalyst weight and moisture content.

3   Results and Discussion

3.1   Structural and textural characterization

The X-ray diffraction patterns of parent and desilicated zeolites exhibit well-resolved peaks representative of the MFI structure; no significant changes in position or intensity of the peaks can be noticed (Figure SI.1). The crystallinity values of the desilicated samples (Table 1) confirm the preservation of the zeolite structure during alkaline treatments; though changes in crystallinity can be appreciated as discussed below. Independently from the treatment conditions, no amorphous phase has been detected; only a slight drop of crystallinity with treatment time was observed. The lowest crystallinity was found for the material treated with NaOH at 80 °C for 5 h, while the TBAOH-treated samples showed slightly higher values of crystallinity. The analysis of the chemical composition for the desilicated zeolites suggests clear differences between NaOH and those obtained by NaOH&TBAOH treatment. Regardless the treatment conditions, i.e. temperature and time, the higher Si/Al ratio values were observed always for samples treated with NaOH&TBAOH. The extent of silicon extraction resulting from the use of different desilicating agents is generally accompanied by changes in crystallinity, i.e. the higher the Si extraction the lower the crystallinity. A similar conclusion has been drawn also for more extensive desilication processes in the case of both medium and high silica zeolites [9,12].

Besides the chemical composition of the bulk, for cracking of large molecules, the composition of the zeolite grains surface is equally important. Thus, the XPS studies of parent and desilicated zeolites were also performed. In the case of the parent zeolite, the Si/Al_{surf} value points out a slightly higher concentration of aluminum atoms on the grain's surface. It is worth mentioning that desilication process proceeds, according to a widely accepted mechanism[33], assuming that silicon atoms in the neighborhood of aluminum atoms are the least prone for extraction during alkaline treatment. Thus the increase in bulk framework aluminum content is expected. Furthermore, for zeolites desilicated using NaOH neither an enhanced silicon extraction nor significant realumination process occurred on the surface during the modification. The Si/Al_{bulk} and Si/Al_{surf} ratios follow the same extent of changes, with only small variations among the samples. This leads to the conclusion that a slightly higher concentration of aluminum atoms on the grain's surface was preserved as it was observed in parent zeolite. On the other hand, for the modified zeolites with NaOH&TBAOH, a more homogenous distribution of silicon and aluminum in the grain volume was found, as it can be derived from the higher similarity in Si/Al_{bulk} and Si/Al_{surf} values. Thus, it seems to be reasonable to assume that in comparison to the NaOH-treated samples, an enhanced silicon extraction from the bulk of the zeolites treated with NaOH&TBAOH took place. It is important to underline that the presented results can only be referred to changes in the composition of the bulk and grains surface, not necessarily to the mesopores surface created during desilication. The enrichment of the grain's surface in aluminum observed for the parent and all modified samples can be responsible for the better catalytic performance in reactions involving branched molecules. However, it cannot be excluded that besides the inhomogeneous nature of the parent sample, also the realumination process is responsible for the enrichment of the grain's surface in aluminum, known as Al-rich shell. Further discussion on the presence of different types of centers originating from the aluminum sites either on the surface or in the zeolite framework will be done with respect to the FTIR studies using different probe molecules (see Section 3.2).

Table 1. Chemical composition of the bulk and surface, crystallinity and textural properties derived from low temperature N_2 physisorption of the parent and desilicated ZSM-5 zeolites.

	Si/Al$_{bulk}$ [a]	Al [a] /$\mu mol \cdot g^{-1}$	Si/Al$_{surf}$ [b]	Cryst. /%	S$_{BET}$ /$m^2 \cdot g^{-1}$	V$_{micro}$ /$cm^3 \cdot g^{-1}$	V$_{meso}$ /$cm^3 \cdot g^{-1}$	S$_{meso}$ /$m^2 \cdot g^{-1}$
ZSM-5/32	32	478	25	100	377	0.17	0.06	40
ZSM-5/32 desil. NaOH@65 C, 0.5 h	20	741	14	87	454	0.16	0.21	145
ZSM-5/32 desil. NaOH@80 C, 0.5 h	18	819	15	86	446	0.15	0.20	135
ZSM-5/32 desil. NaOH@80 C, 5 h	18	819	14	90	435	0.15	0.28	98
ZSM-5/32 desil. NaOH&TBAOH@65 C, 0.5 h	24	622	20	89	415	0.12	0.20	175
ZSM-5/32 desil. NaOH&TBAOH@80 C, 0.5 h	22	676	20	88	383	0.09	0.23	193
ZSM-5/32 desil. NaOH&TBAOH@80 C, 5 h	23	648	19	94	405	0.10	0.32	185

[a] Determined by ICP; [b] Determined by XPS.

Equally important to changes in the structural properties are the textural parameters (Figures 1, 2 and Table 1). As a result of desilication, the major changes are observed in mesopore surface area. The development of a mesopore system in the zeolite grains leads to the enhancement of S$_{meso}$ which attains values as high as 145 and 193 $m^2 \cdot g^{-1}$ for samples treated with NaOH and NaOH&TBAOH, respectively, compared to 40 $m^2 \cdot g^{-1}$ for the parent zeolite. Together with the enhancement of mesopore surface area, the desilication process influences also the micropore volume. The alkaline leaching typically leads to a slight drop in the micropore volume which is usually assigned either to deposition of extra-framework material inside the micropores or to the loss of crystallinity. As mentioned above, the structure of the desilicated zeolites was preserved but there is a drop of about 10% crystallinity, thus the observed drop of micropore volume is probably due to: 1) drop in crystallinity and 2) the presence of extra-framework material inside zeolite channels. The development of a mesopore system was also confirmed by the changes in the shape of the N_2 adsorption-desorption isotherms (Figures 1 and 2). For a typically microporous ZSM-5/32 sample, the isotherm represents a type-I in the IUPAC classification, while for the desilicated materials the type-IV of micro/mesoporous materials is observed, displaying a well-defined hysteresis loop. Additionally, the samples treated with NaOH&TBAOH display a wider hysteresis loop in the isotherm with a closure point around p/p$_0$=0.4. This wider hysteresis and abrupt closure point have been related to the presence of constricted mesopores in which nitrogen only can access through micropores or small mesopores of sizes ≤ 4 nm (3.8 nm according to the BJH model); thus the adsorbate is not fully accessible directly from the surface of the crystals. This effect is also observed for the NaOH-treated samples, but it is less remarkable. The pore size distributions furthermore confirm the hierarchical porosity. Apart from higher values of S$_{meso}$ for the NaOH&TBAOH treated samples, another advantage over the NaOH counterparts is the presence of mesopores with more uniform sizes in the range from 3 to 20 nm. NaOH-treated zeolites possess mesopores larger than 10 nm with a broad distribution of sizes between 10 and 40 nm. The presence of small amount of mesopore surface area in the parent sample results from the intercrystalline porosity.
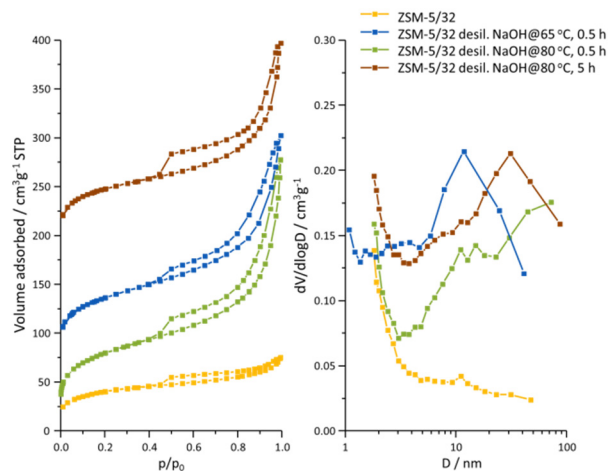
Figure 1. Left) N_2 adsorption-desorption isotherms (shifted upwards for clarity) and right) BJH pore size distributions for the parent and desilicated zeolites, using NaOH.
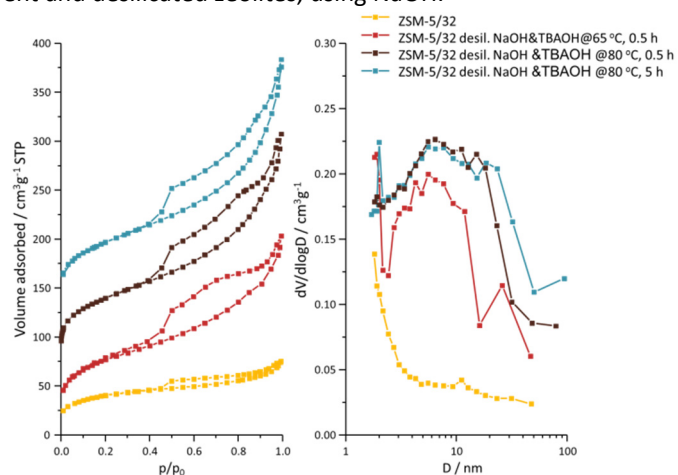

Figure 2. Left) N_2 adsorption-desorption isotherms (shifted upwards for clarity) and right) BJH pore size distributions for the parent and desilicated zeolites, using NaOH&TBAOH.
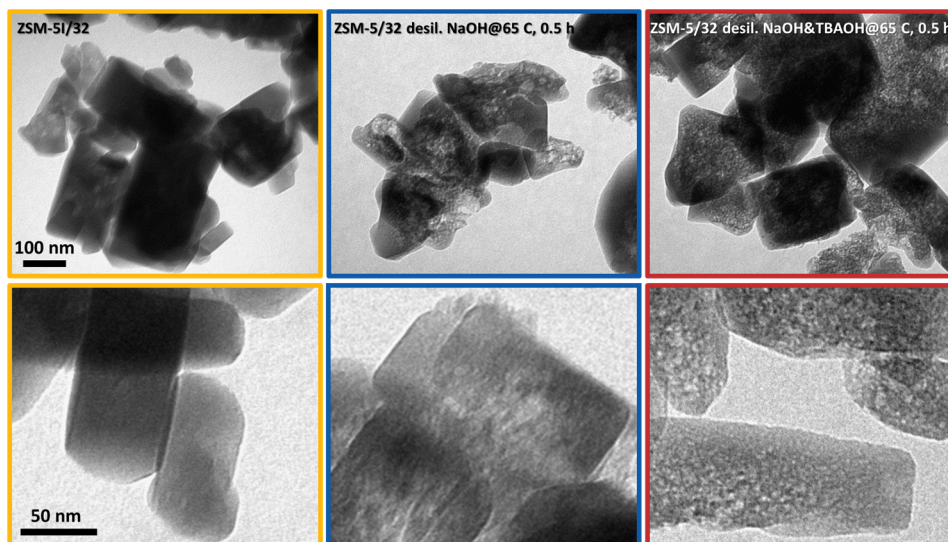

Figure 3. TEM images of the parent (left) and two representative samples treated with NaOH (middle) and NaOH&TBAOH (right), both treated at 65 °C, 0.5 h.

The NaOH or NaOH&TBAOH treatments resulted in a comparable crystallinity, but greatly different micropore volume. One would expect a lower crystallinity could have rendered a lower micropore

volume. The lowered V_{micro} could be related with the presence of amorphous material both as a separate phase and oxidic species. However, no additional peaks or increased background evidencing the formation of an extraframework amorphous phase was found in the XRD patterns, indicating that the size of those species may be too small, beyond the XDR detection limit. The formation of extraframework aluminum species is an inherent feature of desilication. In this study, those moieties were produced in higher amounts in the NaOH&TBAOH-treated materials, as will be evidenced by CO (higher intensity of 2230 cm^{-1} band) and **Py** sorption IR experiments (Section 3.2). The increased Lewis acidity of the desilicated samples, mainly the NaOH&TBAOH-treated ones, is believed to be related to a realumination process on the external surface due to the deposition of previously extracted Al atoms onto the mesopores surface. This is in line with the decreased Si/Al$_{surf}$ values in comparison to Si/Al$_{bulk}$ and enhanced number of Lewis sites available to pivalonitrile (**Pn**) for the mesoporous zeolites. Therefore, though there is no direct proof, the lower V_{micro} is likely related to the micropores blockage by extraframework Al-species.

Additional information on the properties of the generated mesoporosity was drawn from the SEM and TEM images of the parent and two representative zeolites desilicated with NaOH or NaOH&TBAOH (65 °C, 0.5 h) (Figure 3, and Fig. SI.2). The SEM images (Fig. SI.2) evidenced no significant changes in the size or the shape of the grains provoked by desilication. The TEM analysis proved that the desilication process was an effective path for the generation of intraparticle porosity. The NaOH&TBAOH-treatment assured more uniform, across the grain, formation of the mesopores. Leaching with NaOH created mesopores of larger size and more irregularly distributed in the zeolite grains.

3.2 Acidity and accessibility of sites

Investigation of the hydroxyl groups spectra of parent and desilicated zeolites allows for distinguishing four types of bands[12]: the broad band at 3500 cm^{-1} of the silanols nests, the 3605 cm^{-1} band of the acidic Si(OH)Al groups, the 3730 cm^{-1} band of Si(OH) groups in defects and finally the 3742 cm^{-1} Si(OH) groups of silanols on the external surface of the grains and mesopores (Figure 4). The desilication using NaOH and NaOH&TBAOH leads to a visible increase in the intensity of the acidic hydroxyls band. This can be related to the enhanced content of aluminum atoms in the zeolite framework. The significant population enhancement of silanols was concluded from the increased intensity of the 3742 cm^{-1} band and was directly associated with the development of the mesopore system. This found confirmation in the linear dependency between the area of the Si(OH) bands and the mesopore surface area (Figure 5); higher values of mesopore surface area were observed for the samples treated with NaOH&TBAOH, leading to a higher intensity of the Si(OH) bands can be highlighted. Additionally, the 3730 cm^{-1} Si(OH) band, representing silanols in defects, is especially well distinguishable in the case of zeolites treated with NaOH&TBAOH (Figure 4, inset). Thus, together with higher values of S$_{meso}$ it can be concluded that the porosity generated in the zeolites treated with NaOH&TBAOH represents rather the intraparticle character with higher wall curvature, entailing the formation of hydrogen bonded silanols represented by the 3730 cm^{-1} band. Similar conclusion, the dependence between the wall curvature of the mesopores with the type of observed silanols on the mesopores surface, has been pointed out for SBA-15 materials[34]. Finally, it is worth mentioning that, independently from the desilicating agent, the alkaline treatment results in the removal of highly linked silanols in so-called silanols nests represented by the 3500 cm^{-1} band. The preferential removal of silicon depending on the type of neighboring atoms has been already studied

by IR and NMR methods[14]. It has been proven that the aluminum presence has a protective influence on the neighboring silicon atoms.
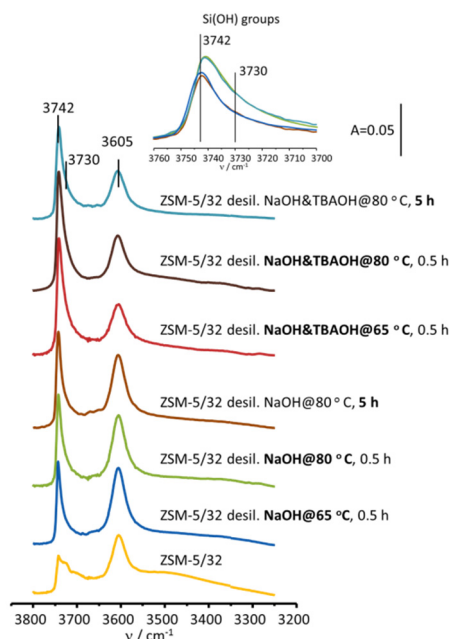

Figure 4. IR spectra of the OH groups for the parent and desilicated ZSM-5 zeolites. Si(OH) groups for selected zeolites are given in the inset.
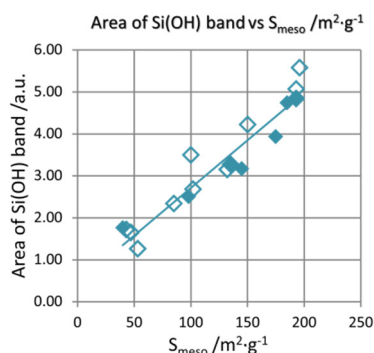

Figure 5. Area of the Si(OH) band region (3780-3680 cm^{-1}) of the desilicated ZSM-5 zeolites (reported in this study (◆), not reported herein[12] ◇) as a function of the mesopores surface area.

Pérez-Ramírez et al.[23] postulated that the Al extracted from the zeolite in alkaline solutions can be partially integrated into the zeolite, giving rise to both Brønsted and Lewis acid sites, as proved by **Py** sorption studies. The origin of the Brønsted acidity was ascribed to Al only partially integrated into zeolite framework but not giving rise to Si(OH)Al groups band in the IR spectra. Furthermore, it has been shown that Al atoms from realumination process, in hierarchically structured zeolite ZSM-5, are able to form protonic sites[23]. However, the majority of these sites upon calcination dehydroxylate easily forming Lewis acid sites[9]. The stoichiometry of dehydroxylation observed for the protonic sites in desilicated zeolites was found to be always 1:1 and to be different from dehydroxylation of typically zeolitic Si(OH)Al groups, where two Si(OH)Al condensate forming one Lewis acid site and water molecule[35]. It should be noted that the same stoichiometry of dehydroxylation (1:1) was reported for amorphous aluminosilicates[36] (MCM-41, MCM-48 and others). The enhancement in the Si(OH)Al band intensity at 3605 cm^{-1} should be ascribed to the overall increase of the content of framework aluminum in the desilicated zeolites. These sites are supposed to originate from tetrahedrally coordinated bulk framework aluminum species preserved during the desilication. The

highly selective removal of Si from the zeolite framework, during alkaline treatment, leads to a better preservation of Al-rich zones in zeolite grains and an overall increase in the framework aluminum content.

Further characteristic features of the acidic sites for the parent and desilicated zeolites involve FTIR quantitative studies of pyridine (0.57 nm), pivalonitrile (0.65 nm) and collidine (0.74 nm) sorption. The use of probe molecules with different kinetic diameter assures the comparison of the changes not only in acidity but also in accessibility of the acid sites after the desilication process. The total concentrations of Brønsted and Lewis acid sites were determined by quantitative IR studies of pyridine as a probe molecule. As it can be noticed (Table 2) the desilication process leads to an increase of the concentration of both Brønsted and Lewis acid sites. With respect to changes in acidity after desilication, the most prominent changes were recognized for the samples treated with NaOH only, in line with the most significant changes in the Si/Al ratios. The total concentrations of acid sites ($C_B + C_L$) determined by pyridine adsorption correspond well to the values of the Al content obtained from the chemical analysis. The differences were <6%; thus it can be deduced that each Al atom is able to form either an acidic Si(OH)Al group or a Lewis acid site, both easily accessible by the **Py** probe molecule.

Table 2. Concentration of aluminum (ICP) and Brønsted and Lewis acid sites interacting with pyridine, pivalonitrile and collidine probe molecules in the parent and desilicated ZSM-5 zeolites

	Al /μmol·g^{-1}	PyH$^+$ /μmol·g^{-1}	PyL /μmol·g^{-1}	$C_B + C_L$^{a} /μmol·g^{-1}	PnH$^+$ /μmol·g^{-1}	PnL /μmol·g^{-1}	Coll /μmol·g^{-1}	$\Delta\nu_{CO..OH}$ /cm^{-1}
ZSM-5/32	478	450	30	480 (0.4)	54	7	22	315
ZSM-5/32 desil. NaOH@65 C, 0.5 h	741	575	205	780 (5.3)	187	92	100	305
ZSM-5/32 desil. NaOH@80 C, 0.5 h	819	630	180	810 (-1.1)	122	49	137	306
ZSM-5/32 desil. NaOH@80 C, 5 h	819	677	111	788 (-3.8)	151	63	124	307
ZSM-5/32 desil. NaOH&TBAOH@65 C, 0.5 h	622	480	160	640 (2.9)	218	106	120	312
ZSM-5/32 desil. NaOH&TBAOH@80 C, 0.5 h	676	545	132	677 (0.1)	316	130	219	309
ZSM-5/32 desil. NaOH&TBAOH@80 C, 5 h	648	511	160	671 (3.5)	221	93	118	310

^{a} *Values in parenthesis are the % difference between ICP and IR studies: $(Al^{ICP}-Al^{B+L})/Al^{ICP} \times 100$*
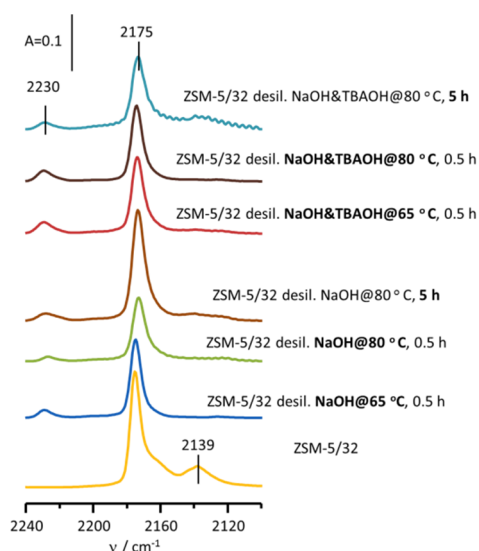

Figure 6. IR spectra of CO sorption at -100 °C for the parent and desilicated ZSM-5 zeolites

The CO sorption studies provide insight into the nature and strength of both Brønsted and Lewis acid sites. The CO adsorbed on the studied zeolites show two bands: the 2175 cm^{-1} band of CO hydrogen bonded to the Si(OH)Al groups[37] and the 2230 cm^{-1} band originating from the interaction of CO with Lewis acid sites of high strength formed in the dehydroxylation process[37] (Figure 6). The band at 2139 cm^{-1} is related to physisorbed CO phase[37]. Since the enhancement of the Brønsted acid sites strength, in the presence of extra-framework electron acceptor acid sites, has been widely reported[38,39] the highest contribution of Lewis acid sites observed for the NaOH&TBAOH-treated sample would guarantee an enhancement in its catalytic performance.

Cracking of large and branched molecules requires not only the tuned acidity but also the enhanced accessibility of the sites. Thus, the IR studies involving the sorption of pivalonitrile and collidine were performed. It can be seen from the results presented in Table 2 that the desilication ensured an enhanced accessibility of the acid sites; this is especially well seen for the samples treated with NaOH&TBAOH. The use of pivalonitrile as probe molecule allows for assessing the number of acid sites accessible from the external surfaces of the grains, the mesopores and from the pore mouths of the micropores. For pivalonitrile, the accessibility of Brønsted acid sites is maintained at a level of ~25% (19-32%) and ~50% (43-58%) for NaOH and NaOH&TBAOH treated samples respectively. This manifests that the alkaline treatment performed in the presence of TBAOH assured superior properties of the obtained materials over these obtained with NaOH only. Besides, the results concerning the accessibility of Lewis acid sites allow for drawing other conclusions. Despite the lower Si/Al$_{surf}$ values for samples treated with NaOH, the accessibility of both protonic and aprotonic sites is distinctly lower than for the NaOH&TBAOH-treated zeolites. This may suggest that for the NaOH&TBAOH samples the majority of sites are accessible from the intraparticle mesoporous surface, being outside of the detection limit for the XPS method. The high values of accessibility of Lewis acid sites confirm their high dispersion on the surface of the mesopores. These highly dispersed Lewis acid sites, of high strength as concluded from CO sorption studies, are expected to have a positive influence on the catalytic activity.

The assessment of the accessibility of the Brønsted acid sites was also performed by IR spectroscopic studies of collidine sorption (Table 2). This probe molecule having a larger kinetic diameter can interact only with the sites located on the more external surface area. Again the higher accessibility of the acid sites is recognized for the samples treated with NaOH&TBAOH. While for the samples treated with NaOH, the accessibility of acid sites for collidine reaches 22%, the NaOH&TBAOH-modified zeolites allow for an enhancement of the accessibility up to 40%. An exception occurs for the harsher employed conditions (5 h treatment) where similar accessibilities were observed for both base treatments. This can be related to the Al-rich shell located in the outer of the zeolite grain, as indicated by XPS results, in combination with the pore restrictions shown in the N$_2$ physisorption experiments, desorption branch with a low closure point. The Al-shell was demonstrated by Groen et al.[40]

The dependency of the accessibility factors for pivalonitrile and collidine as probe molecules with respect to the mesopores surface area is represented in Figure 7. The accessibility factors (AF$_{Pn}$ and AF$_{Coll}$) were defined as the ratio of acid sites concentration accessible to each bulky molecule (collidine or pivalonitrile) to the total concentration of acid sites measured by pyridine sorption [30,41]. The accessibility of acid sites for both probe molecules, as shown in Figure 7, proves a clear correlation with the mesopore surface area. Such an enhanced accessibility of the acid sites was

confirmed in the cracking of TIPB (Section 3.3) and polyethylenes cracking (Section 3.4). In general, the AF_{coll} were lower than AF_{Pn} for equal S_{meso}, which is due to the larger kinetic diameter of **Coll** with respect to **Pn**. Thus the AF_{coll} accounts for the less accessible acid sites.
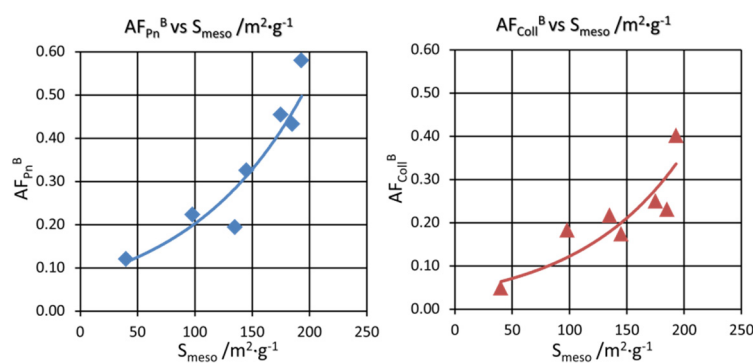

Figure 7. Accessibility factors for (left) pivalonitrile (◆) and (right) collidine (▲) as probe molecules as a function of the mesopores surface area of the parent and all desilicated ZSM-5 zeolites.

The last aspect of the acidity characterization concerns the determination of acid sites strength. Similarly, as the accessibility features, the acid sites strength should also find a direct reflection in the catalytic cracking performance of the studied zeolites. Information on the changes in the acid strength was derived from the values of the frequency shifts $\Delta\nu_{CO..OH}$ of the band of the Si(OH)Al groups interacting with the CO molecule (Table 2). The desilication process led to noticeable changes in the strength of Si(OH)Al groups: a drop of $\Delta\nu_{CO..OH}$ is clearly visible. This decrease in the acid strength of the protonic sites can be related to (i) the decrease of Si/Al ratio of the desilicated zeolites and (ii) to the extraction of Al atoms from the most acidic Si(OH)Al groups due to their low stability in tetrahedral framework positions. Such an interpretation has been proposed in our earlier study of desilicated BEA zeolites[42] and is also discussed in the work of Lee et al.[43], reporting a considerable reduction of the amount of strong acid sites after the introduction of mesopores in the ZSM-5 zeolite. The changes in the acid strength upon desilication will be also discussed with regard to the catalytic cracking reactions (Section 3.3).

3.3   Catalytic performance in *n*-decane and TIPB cracking probe molecules

The cracking reactions of TIPB (1,3,5-tri-iso-propylbenzene) and *n*-decane were performed in order to evaluate the impact of the textural and acidic properties resulting from desilication on the catalytic performance; the changes are compared to the untreated ZSM-5 zeolite. Three catalytic parameters were evaluated: conversion at various oil/cat ratios, coke content, and kinetic constant. The catalytic activity in the cracking of TIPB, a branched and bulky molecule (kinetic diameter 0.95 nm) being not able to penetrate the 10-MR channels of ZSM-5 zeolite, should reflect the alterations in the textural parameters followed by the changes in the accessibility of the acid sites. On the other hand, the activity in the catalytic cracking of *n*-decane is expected to reflect the changes in the intrinsic Brønsted acidity. The cracking of *n*-decane, able to freely diffuse through the micropores, is highly demanding on the concentration and the strength of the acid sites. The desilicated ZSM-5 zeolites were supposed to overcome the limitations of the microporous counterpart demonstrating the same trends as observed in the FTIR and textural studies results. The samples treated under NaOH and NaOH&TBAOH at 65 °C for 0.5 h were the most representative examples of the desilicated zeolites and will be further discussed in this section.
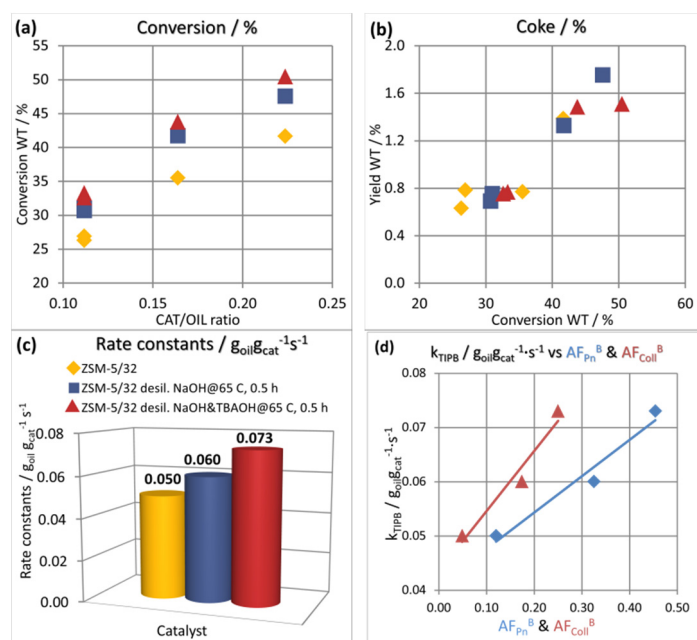
Figure 8. (a) Conversion, (b) coke yield, (c) rate constants (k_{TIPB}) from the TIPB catalytic cracking at 500 °C and 60 s time on stream over the parent and desilicated ZSM-5 zeolites and (d) rate constant (k_{TIPB}) from the TIPB catalytic cracking as a function of the accessibility factors for pivalonitrile and collidine probed Brønsted sites.

The catalytic activity in the cracking of TIPB over the parent zeolite and those desilicated with the use of NaOH or NaOH&TBAOH showed an enhancement of the conversion for the modified materials (Figure 8a). A strong correlation is observed between catalytic activity of the hierarchical ZSM-5 zeolites and their textural properties, i.e. the mesopore surface area and the mesopore volume, as well as the accessibility of the acid sites have a positive impact on the conversion levels at various cat/oil ratio. It can be noticed that the highest catalytic activity is observed for the sample treated with NaOH&TBAOH. This fact further supports the conclusions withdrawn from the textural parameters and FTIR studies, which point out on a superior type of mesoporosity, characterized by smaller size and a narrower diameter distribution. As mentioned, the catalytic activity can be also associated with the accessibility factors of the acid sites estimated from pivalonitrile and collidine molecules; the observed order of increasing conversion correlates with the enhancement of the accessibility factors. The micro/mesoporous character of the desilicated zeolites allow for a similar formation of coke deposit at higher conversion in comparison to the parent zeolite (Figure 8b).

The catalytic activity was also evaluated on the basis of rate constants, which demonstrate the same order of increase as the accessibility factors and mesopore surface areas (Figure 8c). This is shown in Figure 8d where the reaction rate constants are linearly dependent with the accessibility factors for pivalonitrile and collidine. The highest k_{TIPB} value is observed for the NaOH&TBAOH-treated zeolite. In spite of the drop of acid strength, the generation of the secondary system of mesopores leads to the higher accessibility of the protonic sites for TIPB. As the catalytic activity increased with the accessibility of **Coll** protonic sites, it could be anticipated that the mesopores system promoted the diffusion of the bulky 1,3,5-triisopropylbenzene and, finally, provided higher activity of the hierarchical zeolites. Therefore, not only the acidity of the protonic sites but their improved accessibility is evidenced in Fig. 8d as predominant factors influencing the TIPB cracking. It has to be remarked that the mesoporous ZSM-5 zeolite obtained by NaOH&TBAOH treatment showed a high activity for the cracking of TIPB despite the presence of constricted mesoporosity, as indicated by the nitrogen desorption isotherms. These mesopores of ink-bottle shape, when reported for the

conversion of methanol to hydrocarbons[44] did not improve the lifetime. The reaction temperatures for TIPB cracking (500 °C) are higher than those applied for the methanol to hydrocarbon reaction (400 - 450 °C). Thus for the cracking of TIPB, i.e. reaction very sensitive to the presence of mesopores, the mesoporosity is active, what suggests that at least part of the mesopore system is accessible. An important observation is the fact that a 4-fold increase of mesopore surface area for the desilicated samples delivers an enhancement of the rate constants up to 40% only. This suggests the presence of restricted porosity, possibly induced by the Al-rich shell, in addition to the lower acid strength of the sites for the ZSM-5 zeolite with Si/Al=32. An opposite effect was reported for highly siliceous zeolite ZSM-5 (Si/Al=164), where the formation of the Al-rich shell is less probable[9,27]. Thus the influence of mesoporosity for high silica ZSM-5 (Si/Al=164) has a higher impact on the catalytic performance, e.g. rate constants of the TIPB cracking. The enhanced activity of highly siliceous ZSM-5 (Si/Al=164) was interpreted not only by the developed mesopore surface area but also by the high acid strength of the sites due to the high Si/Al ratio.

The catalytic activity of ZSM-5 zeolites in the cracking of n-decane, with a kinetic size enabling non-restricted diffusion through the 10-MR channels, is mainly determined by the concentration and strength of Brønsted acid centers[45,46]. Indeed, the desilication process leading to a drop of the strength of the acid sites also causes a decrease in the conversion of n-decane cracking (Figure 9a). This effect is especially pronounced for the zeolite treated with NaOH only, for which a 10% of decreased conversion was recognized. Among the desilicated NaOH&TBAOH-treated materials, the drop of both the acid strength and the conversion is less significant. A lower strength of the acid sites was proven in the CO sorption FTIR studies, discussed previously (Section 3.2), compared to the parent zeolite. The observed decrease in the conversion demonstrates that despite the enhanced concentration of the protonic sites, the acid strength is a determining factor for the activity in the cracking of n-decane. The process of catalytic cracking of n-decane takes place mainly in the micropore system, thus the presence of mesopores can limit the confinement effect and negatively influence the activity of the catalytic cracking[47]. Despite the generation of a significant mesopore surface area through the desilication process, the amount of formed coke deposits for n-decane cracking is being maintained, or slightly higher, than the parent zeolite (Figure 9b). Additionally, Lewis acid sites have been considered as active species playing a role in the formation of carbonaceous deposits during the catalytic reaction[48,49]. The same trend as for conversion is also seen for the experimentally determined rate constants, what further confirms the drawn conclusions (Figure 9c). Clearly visible are the advantages of the NaOH&TBAOH over the NaOH treatments; still, the highest performance is observed for the parent zeolite.
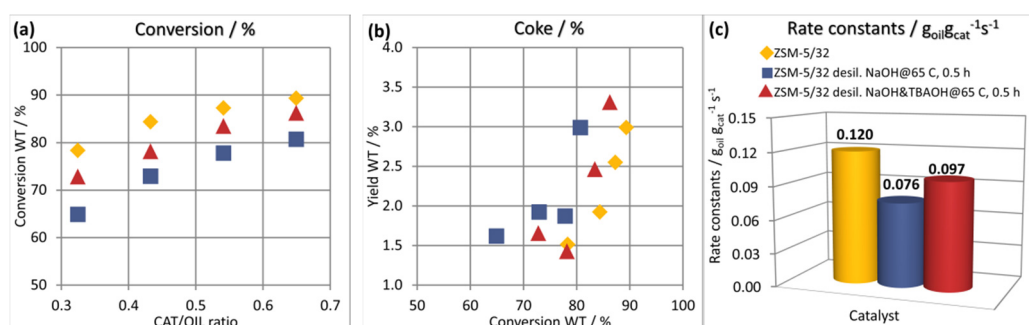

Figure 9. (a) Conversion, (b) coke yield and (c) rate constants (k_{n-C10}) from the n-decane catalytic cracking at 500 °C and 60 s time on stream over parent and desilicated zeolites

These findings clearly demonstrate the influence of desilication process on the catalytic performance of hierarchical zeolites. It can be expected that the cracking of large and bulky molecules over hierarchical zeolites will proceed more effectively than over their microporous counterparts. On the other hand, for reactions requiring the presence of strong acid centres a drop in activity is expected.

Moreover, the increase in the accessibility of the acid sites improves the selectivity of the cracking reactions. In fact, for both *n*-decane and TIPB cracking, hydrogen transfer reactions were reduced. The hydrogen transfer processes as secondary reactions that consume olefins are expressed by the propene/propane ratio (Fig. 10); this is higher especially in the case of the sample treated with NaOH&TBAOH at high conversion. With the improvement in the mesoporosity, the effective path through the microporous channels is shortened and the effect of secondary reactions is lowered, resulting in a higher olefin selectivity.
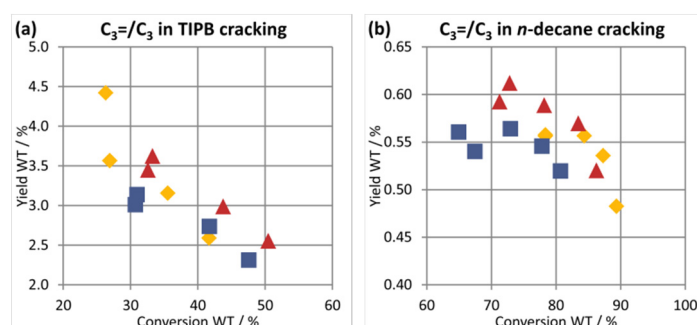

Figure 10. The propene/propane ratio for cracking reactions of (a) TIPB and (b) *n*-decane in case of the parent ZSM-5/32 zeolite (◆), desilicated ZSM-5/32 desil. NaOH@65 C, 0.5 h (■) and ZSM-5/32 desil. NaOH&TBAOH@65 C, 0.5 h (▲) zeolites.

3.4 Catalytic performance in LDPE and HDPE cracking processes

Catalytic degradation of PEs over zeolites at first stage reacts with the active sites on the external surface of the zeolite grains, as its kinetic diameter is significantly larger than the pore entrance in the zeolite structure. After the preliminary reactions on the outer surface, the partly degraded products which are able to diffuse into the micropores of the zeolite are subsequently cracked at the pore entrance; then they further react on the acid sites located inside the micropores. Thus, the strength of acid sites accessible from the external surface and those situated inside micropores are both relevant, and together with the pore structure of the zeolite influence the cracking reaction activity and selectivity [50,51].

The results of LDPE catalytic cracking over the parent and hierarchical ZSM-5 zeolites as a function of temperature are presented in Figure 11. It can be noticed that the conversion curves for all the hierarchical zeolites are shifted to lower temperatures with respect to microporous parent zeolite. For the LDPE cracking, the complete conversion for all the studied zeolites, parent and modified, is obtained at temperatures lower than 400 °C. The highest activity is found for samples treated with NaOH&TBAOH demonstrating lower values of $T_{5\%}$ and $T_{50\%}$ i.e. temperatures necessary for 5% and 50% of LDPE conversion. These results are in agreement with the acidic and textural properties. Among the mesostructured zeolites, the materials modified with NaOH&TBAOH demonstrated a higher acid density, high acid strength (compared to the NaOH treatment) with an enhanced mesoporosity.

The cracking of HDPE over the studied ZSM-5 zeolites (Figure 12) required higher temperatures than for LDPE, what can be associated with the linear character of the HDPE structure. The absence of branching which are precursors of tertiary carbocations negatively affects its susceptibility to the cracking reactions[18]. The highest activity in the HDPE cracking is observed again for samples treated with NaOH&TBAOH. The temperatures for 5% and 50% conversions are about 53 °C and 19 °C lower, respectively, than for the parent material. It is worth mentioning that the sample treated with NaOH (5h, 80 °C) presents a distinctly lower activity than the other zeolites, either parent or modified ones. This lowered activity can find the explanation both in the textural and the acidic parameters. After the modification with NaOH for a prolonged time and at high temperature (5h, 80 °C) the drop of the acid strength, and restricted pores can entail the activity reduction (Table 1 and 2). On the other hand, the materials treated with NaOH&TBAOH are characterized by a higher strength of the acid sites (compared to the NaOH treatment) and highly developed mesoporous surface with narrower pore size distribution, in comparison to those treated with NaOH only. It is necessary to underline that the desilication with NaOH&TBAOH mixture caused significantly enough changes in acidity (strength and density of accessible sites for **Pn** and **Coll**) and porosity to prompt the activity in the LDPE and HDPE cracking reactions. Thus the superior performance of the NaOH&TBAOH-modified materials over the parent and NaOH-treated materials results from the higher population of acid sites, with intermediate strength, and the development of the external surface area leading to the enhanced catalytic degradation rate[52].
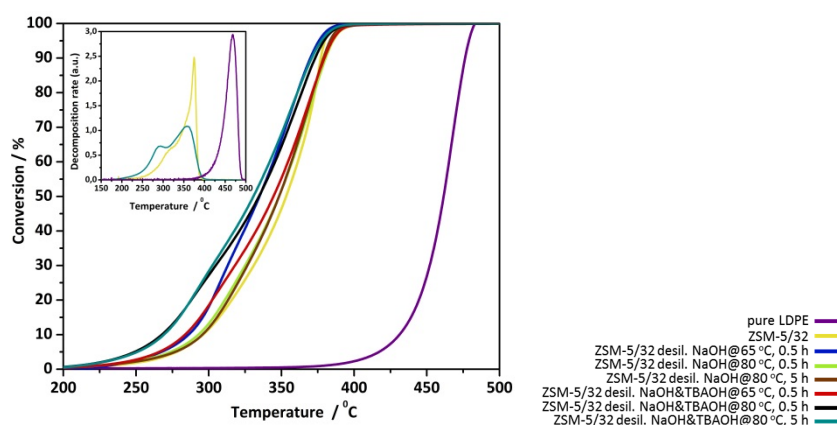

Figure 11. Results of LDPE catalytic cracking conversion as a function of temperature over the parent and desilicated ZSM-5 zeolites; decomposition rate of LDPE over selected samples (inset)
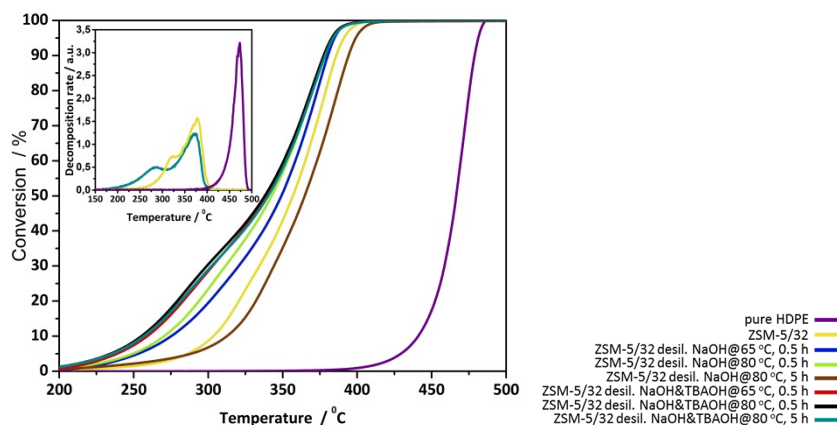

Figure 12. Results of HDPE catalytic cracking conversion as a function of temperature over the parent and desilicated ZSM-5 zeolites; decomposition rate of HDPE over selected samples (inset)

It is known that the early stage of PE cracking reaction begins with the hydride abstraction or addition of a proton to C–C bond, thus the zeolite of a higher acid strength accessible through mesopores produce more active alkylcarbenium or alkylcarbonium ions at the early stage of the reaction[53]. At higher temperature and conversion PEs undergo substantial cracking, and the diffusion of smaller counterparts is improved. This ''leveling effect'' becomes predominant over the acid strength at temperatures as high as 350 $^{\circ}$C, where all zeolites demonstrated a more similar activity.

When observing the conversion curves (Figs. 11 and 12), for the LDPE there are some differences between the catalysts and these may be related to meso/macroporosity differences of the external surface. The major differences are however noticed with the linear HPDE and low conversion, while at higher conversion the differences vanish. This can be quantified and evaluated. The influence of site accessibility on the catalytic activity is seen as a dependency between the estimated values of AF_{Pn} or AF_{Coll} and the temperatures for 5% and 50% conversion ($T_{5\%}$ and $T_{50\%}$, resp.), in Figure 13 and 14. Linear correlations are found for both LDPE and HDPE with **Pn** and **Coll**. Generally speaking, the correlations in Fig. 13 and 14 demonstrate that the enhanced amount of the pore mouths is responsible for increased activity in LDPE and HDPE cracking. The increasing accessibility of the acid sites leads to an enhanced cracking activity, as observed by a decrease of the $T_{5\%}$ and $T_{50\%}$. It is found that the accessibility of the acid sites has a privileged influence on activity at lower temperatures. The differences in the slope of linear dependency between the temperatures for both 5% and 50% conversion, and the accessibility of the acid sites, are observed depending on the type of cracked polyethylene. Cracking reactions of HDPE performed over the hierarchical zeolite seem to be more influenced by the accessibility factors (i.e. more improved by the presence of mesopores) than it is seen for LDPE cracking. In other words, the LDPE is less influenced by the accessibility. This can be related to the various degree of branching of HDPE and LDPE. Since the HDPE possess a linear structure, it can penetrate easily and make use of the available mesoporosity for the early-stage cracking (reflected in the $T_{5\%}$); therefore low conversion (e.g. $T_{5\%}$) is more affected by the enhanced amount of pore mouths of ZSM-5 channels on the mesopores. High degree of branching, i.e. large amount of short hydrocarbon chains, typical for LDPE induces a more constrained access to the pore entrances. Thus the generation of the secondary mesoporosity in the studied zeolites does not influence the conversion of LDPE as significantly as it was observed for HDPE. The influence of the $T_{50\%}$ with the accessibility factors for HDPE and LDPE is weaker than for $T_{5\%}$; this suggests that the cracking at this conversion involves intermediate molecules of smaller size with less diffusional limitations.

The performance for the LDPE and HDPE, could not be enhanced much by playing with the desilication conditions using NaOH&TBAOH, which gave the highest external surface area. One would be expecting a higher conversion that could be optimized with the zeolite treatment conditions. This can be related to the possible Al-rich shell that is formed at the external part of the zeolite grains displaying narrower entrances, which has been claimed that hinders the reaction.[40] With respect to our prior work[27], this high-Al zeolite with enhanced mesoporosity via NaOH&TBAOH treatment in the polyolefins cracking gave the most pronounced differences with respect to the native zeolite.
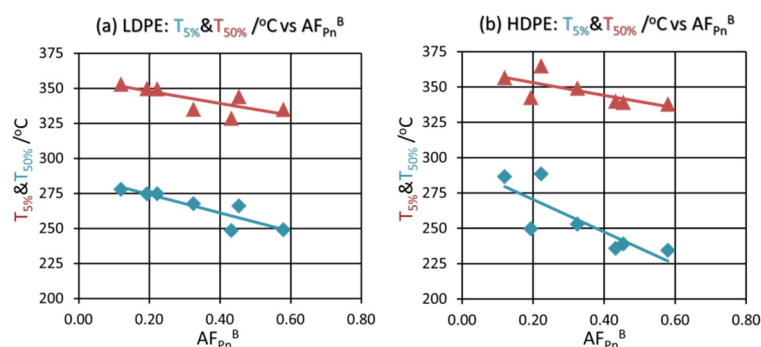
Figure 13. Temperatures for 5% and 50% conversion ($T_{5\%}$ ▲ and $T_{50\%}$ ◆) for (a) LDPE and (b) HDPE cracking plotted against the accessibility factor values for the Brønsted acid sites estimated from pivalonitrile (AF_{Pn}^B) sorption experiments.
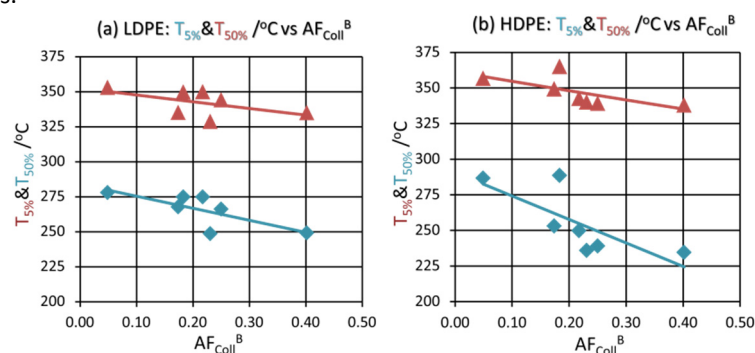

Figure 14. Temperatures for 5% and 50% conversion ($T_{5\%}$ ▲ and $T_{50\%}$ ◆) for (a) LDPE and (b) HDPE cracking plotted against the accessibility factor values for the Brønsted acid sites estimated from collidine (AF_{Coll}^B) sorption experiments.

4   Conclusions

The effectiveness of hierarchical zeolites (Si/Al = 18 - 32) in acid catalyzed cracking of TIPB, n-decane and polyethylenes was evaluated in the terms of their accessible acidity and generated mesoporosity. The cracking of large and bulky molecules (TIPB versus n-decane) over the hierarchical zeolites proceeded more effectively than over their microporous counterparts, and this was correlated to the collidine and pivalonitrile accessibility factors. The n-decane cracking reveals that the acid strength is the most dominating factor, pointing out that the NaOH&TBAOH treatment gave stronger sites than NaOH, but lower than the native zeolite. During the n-decane and TIPB cracking, hydrogen transfer reactions were reduced, for the NaOH&TBAOH materials due to the shorter path through the microporous channels, resulting in a higher olefin selectivity. A similar behavior than TIPB was observed for the cracking of LDPE and HDPE. Linear correlations of the temperatures for 5% and 50% conversion for LDPE and HDPE with the accessibility factors for branched probe molecules (pivalonitrile and collidine) were found, demonstrating that the enhanced amount of the pore mouths is responsible for increased activity in LDPE and HDPE cracking. At low conversion, linear HDPE is more sensitive by the enhanced mesoporosity, as determined by the steeper $T_{5\%}$ correlation, than branched LDPE. At high conversion the influence of the $T_{50\%}$ with the accessibility factors for HDPE and LDPE is weaker, suggesting that the cracking at this stage involves intermediate molecules of smaller size with less diffusional limitations. The performance for the LDPE and HDPE, could not be enhanced much by tuning the desilication conditions for the NaOH&TBAOH zeolites, which gave the highest external surface area. This can be related to the possible Al-rich shell with narrower entrances which will hinder the reaction. With respect to our prior work, the chosen zeolite and

polyolefins cracking gave the most pronounced differences with respect to the created mesoporosity.
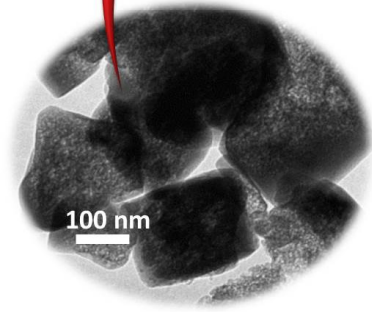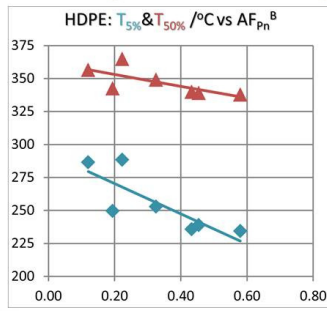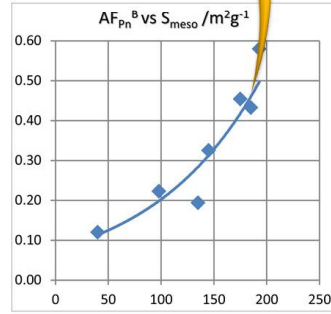
Acknowledgements

References

1. D. Verboekend and J. Perez-Ramirez, *Catalysis Science & Technology*, 2011, **1**, 879-890.
2. K. Gora-Marek, K. Tarach, J. Tekla, Z. Olejniczak, P. Kustrowski, L. Liu, J. Martinez-Triguero and F. Rey, *Journal of Physical Chemistry C*, 2014, **118**, 28043-28054.
3. M. S. Holm, E. Taarning, K. Egeblad and C. H. Christensen, *Catalysis Today*, 2011, **168**, 3-16.
4. Y. Liu, W. Zhang and T. J. Pinnavaia, *Angewandte Chemie International Edition*, 2001, **40**, 1255-1258.
5. I. Schmidt, A. Boisen, E. Gustavsson, K. Ståhl, S. Pehrson, S. Dahl, A. Carlsson and C. J. H. Jacobsen, *Chemistry of Materials*, 2001, **13**, 4416-4418.
6. M. Choi, H. S. Cho, R. Srivastava, C. Venkatesan, D.-H. Choi and R. Ryoo, *Nat Mater*, 2006, **5**, 718-723.
7. H. Wang and T. J. Pinnavaia, *Angewandte Chemie International Edition*, 2006, **45**, 7603-7606.
8. D. Verboekend, M. Milina, S. Mitchell and J. Pérez-Ramírez, *Crystal Growth & Design*, 2013, **13**, 5025-5035.
9. K. Sadowska, K. Gora-Marek, M. Drozdek, P. Kustrowski, J. Datka, J. Martinez Triguero and F. Rey, *Microporous and Mesoporous Materials*, 2013, **168**, 195-205.
10. S. Abelló, A. Bonilla and J. Pérez-Ramírez, *Applied Catalysis A: General*, 2009, **364**, 191-198.
11. M. Müller, G. Harvey and R. Prins, *Microporous and Mesoporous Materials*, 2000, **34**, 135-147.
12. K. Sadowska, K. Góra-Marek and J. Datka, *Vibrational Spectroscopy*, 2012, **63**, 418-425.
13. J. Pérez-Ramírez, D. Verboekend, A. Bonilla and S. Abelló, *Advanced Functional Materials*, 2009, **19**, 3972-3979.
14. K. Sadowska, A. Wach, Z. Olejniczak, P. Kustrowski and J. Datka, *Microporous and Mesoporous Materials*, 2013, **167**, 82-88.
15. D. P. Serrano, J. Aguado and J. M. Escola, *ACS Catalysis*, 2012, **2**, 1924-1941.
16. A. Bonilla, D. Baudouin and J. Pérez-Ramírez, *Journal of Catalysis*, 2009, **265**, 170-180.
17. D. P. Serrano, J. Aguado, J. M. Escola, J. M. Rodriguez and A. Peral, *Journal of Catalysis*, 2010, **276**, 152-160.
18. J. Aguado, J. L. Sotelo, D. P. Serrano, J. A. Calles and J. M. Escola, *Energy & Fuels*, 1997, **11**, 1225-1231.
19. S. Kumar, A. K. Panda and R. K. Singh, *Resources, Conservation and Recycling*, 2011, **55**, 893-910.
20. R. C. Mordi, R. Fields and J. Dwyer, *Journal of Analytical and Applied Pyrolysis*, 1994, **29**, 45-55.
21. P. Castaño, G. Elordi, M. Olazar, A. T. Aguayo, B. Pawelec and J. Bilbao, *Applied Catalysis B: Environmental*, 2011, **104**, 91-100.
22. G. Elordi, M. Olazar, G. Lopez, P. Castaño and J. Bilbao, *Applied Catalysis B: Environmental*, 2011, **102**, 224-231.
23. D. Verboekend and J. Pérez-Ramírez, *Chemistry – A European Journal*, 2011, **17**, 1137-1147.
24. C. S. Cundy and P. A. Cox, *Microporous and Mesoporous Materials*, 2005, **82**, 1-78.
25. C. T. Kresge, M. E. Leonowicz, W. J. Roth, J. C. Vartuli and J. S. Beck, *Nature*, 1992, **359**, 710-712.
26. L. D. Bonifacio, B. V. Lotsch and G. A. Ozin, in *Comprehensive Nanoscience and Technology*, eds. G. D. Scholes and G. P. Wiederrecht, Academic Press, Amsterdam, 2011, pp. 69-125.
27. K. A. Tarach, J. Martinez-Triguero, F. Rey and K. Góra-Marek, *Journal of Catalysis*, 2016, **339**, 256-269.
28. E. P. Barrett, L. G. Joyner and P. P. Halenda, *Journal of the American Chemical Society*, 1951, **73**, 373-380.
29. K. Góra-Marek, M. Derewiński, P. Sarv and J. Datka, *Catalysis Today*, 2005, **101**, 131-138.

30. K. Sadowska, K. Góra-Marek and J. Datka, *Journal of Physical Chemistry C*, 2013, **117**, 9237-9244.
31. K. Mlekodaj, K. Tarach, J. Datka, K. Gora-Marek and W. Makowski, *Microporous and Mesoporous Materials*, 2014, **183**, 54-61.
32. A. Corma and J. Martínez-Triguero, *Applied Catalysis A: General*, 1994, **118**, 153-162.
33. J. C. Groen, L. A. A. Peffer, J. A. Moulijn and J. Pérez-Ramírez, *Chemistry – A European Journal*, 2005, **11**, 4983-4994.
34. D. Majda, K. Tarach, K. Góra-Marek, A. Michalik-Zym, B. D. Napruszewska, M. Zimowska and E. M. Serwicka, *Microporous and Mesoporous Materials*, 2016, **226**, 25-33.
35. J. B. Uytterhoeven, L. G. Christner and W. K. Hall, *The Journal of Physical Chemistry*, 1965, **69**, 2117-2126.
36. K. Góra-Marek, J. Datka, *Applied Catalysis A: General*, 2006, **302**, 104-109.
37. H. Knözinger, in Adsorption on Ordered Surfaces of Ionic Solids and Thin Films: Proceedings of the 106th WE-Heraeus Seminar, Bad Honnef, Germany, February 15–18, 1993, eds. H.-J. Freund and E. Umbach, Springer Berlin Heidelberg, Berlin, Heidelberg, 1993, pp. 257-267.
38. N. O. Gonzales, A. T. Bell, A. K. Chakraborty, *Journal of Physical Chemistry B*, 1997, **101**, 10058-10064.
39. M. Derewiński, K. Góra-Marek, K. Lázár, J. Datka, *Studies in Surface Science and Catalysis*, 2008, **174 B,** 865-868.
40. J. C. Groen, T. Bach, U. Ziese, A. M. Paulaime-van Donk, K. P. de Jong, J. A. Moulijn and J. Pérez-Ramírez, *Journal of the American Chemical Society*, 2005, **127**, 10792-10793.
41. F. Thibault-Starzyk, I. Stan, S. Abelló, A. Bonilla, K. Thomas, C. Fernandez, J.-P. Gilson and J. Pérez-Ramírez, *Journal of Catalysis*, 2009, **264**, 11-14.
42. K. Tarach, K. Gora-Marek, J. Tekla, K. Brylewska, J. Datka, K. Mlekodaj, W. Makowski, M. C. Igualada Lopez, J. Martinez Triguero and F. Rey, *Journal of Catalysis*, 2014, **312**, 46-57.
43. J. Y. Lee, S. M. Park, S. K. Saha, S. J. Cho and G. Seo, *Applied Catalysis B: Environmental*, 2011, **108–109**, 61-71.
44. M. Milina, S. Mitchell, P. Crivelli, D. Cooke and J. Pérez-Ramírez, *Nat Commun*, 2014.
45. A. Corma, P. J. Miguel and A. V. Orchille´s, *Applied Catalysis A: General*, 1994, **117**, 29-40.
46. B. Xu, C. Sievers, S. B. Hong, R. Prins and J. A. van Bokhoven, *Journal of Catalysis*, 2006, **244**, 163-168.
47. A. Corma, F. Melo, L. Sauvanaud and F. J. Ortega, *Applied Catalysis A: General*, 2004, **265**, 195-206.
48. H. G. Karge, eds. H. van Bekkum, E.M. Flanigen, P.A. Jacobs, J.C. Jansen, *Studies in Surface Science and Catalysis*; Elsevier, **2001**, *137*, 707.
49. J. Weitkamp, M. Hunger,eds. J. Čejka, H. van Bekkum, A. Corma, F. Schüth, *Studies in Surface Science and Catalysis*; Elsevier, **2007**, *168*, 787.
50. Y. S. You, J.-H. Kim and G. Seo, *Polymer Degradation and Stability*, 2001, **72**, 329-336.
51. G. Manos, A. Garforth and J. Dwyer, *Industrial & Engineering Chemistry Research*, 2000, **39**, 1198-1202.
52. Q. Zhou, Y.-Z. Wang, C. Tang and Y.-H. Zhang, *Polymer Degradation and Stability*, 2003, **80**, 23-30.
53. H. Zhang, Y. Ma, K. Song, Y. Zhang and Y. Tang, *Journal of Catalysis*, 2013, **302**, 115-125.

Catalytic activity

HDPE: $T_{5\%}$ & $T_{50\%}$ /°C vs AF_{Pn}^B

AF_{Pn}^B vs S_{meso} /m²g⁻¹

Porosity

Accessibility